SLAC–PUB–6380
October 1993
(A)

Experimental Studies of the Charge Limit Phenomenon in GaAs Photocathodes*

H. Tang, R. Alley, H. Aoyagi†, J. Clendenin, P. Saez, D. Schultz, and J. Turner
Stanford Linear Accelerator Center, Stanford University, Stanford, CA 94309

ABSTRACT

GaAs photocathodes have been in use for generating high intensity polarized electron beams (up to a peak current of 6 A in 2 ns pulses) for the SLC high energy physics program. If the quantum efficiency (measured at low light intensities) of a GaAs photocathode is below a certain level, the maximum photoemitted charge is found to be limited by the intrinsic properties of the cathode instead of by the space charge limit. We have studied this charge limit phenomenon in a variety of GaAs photocathodes. The effects of the quantum efficiency, excitation laser wavelength, and extraction electric field on the charge limit have been examined. The temporal behavior of the charge limit as manifested in both intrapulse and interpulse effects has also been studied. These results will be discussed in light of possible mechanisms.

Polarized electrons generated by photoemission from negative electron affinity (NEA) GaAs cathodes with circularly polarized light have been in continuous use for the SLC high energy physics programs at SLAC since the spring of 1992 [1,2]. The demand for the highest possible polarization of the electron beam dictates that the energy of the excitation photons must be very close to the band gap energy of the cathode material. Operating under such a condition revealed a new phenomenon in the physics of photoemission from NEA semiconductor cathodes — if the quantum efficiency (QE) of the cathode is below a certain level the total charge extractable from a cathode within a short pulse (on the order of a few nanoseconds) saturates to a limit that is less than what the space charge limit permits [3,4]. As the beam intensity requirement is very high for the SLC/SLD program, and surely even more so for future linear colliders, this charge limit effect imposes a significant constraint on the usability of NEA photocathodes. We report in this note a systematic study on the charge limit phenomenon.

The experiments were conducted by using the Gun Test Facility at SLAC. The facility consists of a 20 mm cathode aperture diode gun with a loadlock system for easy cathode change, two pulsed Ti:Sapphire lasers pumped by a frequency-doubled Nd:YAG laser, and an electron beamline terminating into a Faraday cup. The two Ti:Sapphire lasers are tuned to 865 nm and 775 nm, respectively, and have a FWHM of about 2 nanoseconds. Their spot sizes are adjusted to >20 mm so that the cathode is fully illuminated in the charge limit studies. Two low power cw diode lasers of 752 nm and 833 nm, respectively, are used for quantum efficiency measurements with a spot size of 14 mm centered on the cathode. An optically isolated nanoammeter, a beam position monitor (BPM), and a gap monitor are used for beam intensity measurements. Unless otherwise stated, the cathode is always biased at –120 kV and maintained at a temperature of –5 ± 2 °C. The cathode activation method consists of heat cleaning to 600 °C for 1 hour, Cs application until the photoyield peaks, and finally Cs and NF_3 codeposition until the photoyield maximizes. The vacuum in the gun is maintained at about 1×10^{-11} Torr by means of ion and nonevaporative getter pumping. A large number of strained and unstrained GaAs cathodes have been studied. In the following we shall focus our attention on two 300 nm strained GaAs

*Work supported by the Department of Energy under contract DE-AC03-76SF00515

Presented at the Workshop on Photocathodes for Polarized Electron Sources for Accelerators, Stanford Linear Accelerator Center, Stanford, CA, September 8–10, 1993

cathodes doped with Zn to a concentration of 5×10^{18} cm^{-3} and 2×10^{19} cm^{-3}, respectively, which will hereafter be referred to as cathode 1 and cathode 2.

Before discussing the experimental results, consider an ideal case in which the photocathode is assumed to respond linearly to light illumination. Figure 1 illustrates in a simplistic fashion the charge versus light pulse energy behavior for two temporal forms of light pulses, square pulses and Gaussian-like pulses. For square pulse light illumination, the charge pulse is also square, and its amplitude increases linearly with light pulse amplitude, or energy, and eventually saturates to the space charge limit. The corresponding saturation curve is very simple, consisting of a straight line with a slope corresponding to the quantum efficiency and a zero slope line in the space charge limit region. For Gaussian-like light pulses, the charge pulse initially follows the shape of the light pulse, and changes to a truncated, or flat-topped, Gaussian-like pulse when its maximum amplitude exceeds the space charge limit. The total charge keeps increasing with increasing light pulse energy even in the space charge limit region due to increased contribution from the leading and trailing edges of the light pulse. This case is more relevant to our experimental study because our laser pulses, as shown in Figure 2, is Gaussian like.

Figure 3 shows a typical charge saturation plot and several charge pulses at various laser pulse energies measured with the gap monitor for cathode 1. The saturation plot is characterized by a nearly linear response of the cathode to the laser pulses in the low energy region, and increasingly nonlinear behavior as the laser energy further increases. The maximum charge is much less than the space charge limit, which is in excess of 16×10^{10} electrons/pulse, and the saturation curve is also drastically different from the space charge limit case as illustrated in Figure 1(b). Further increase in laser energy in the charge limit region results in a decrease in the photoemitted charge. The charge pulses shown in the lower panel reveal that as the charge limit sets in, the later portion of the charge pulse becomes suppressed. As a result, the charge pulse becomes narrower and peaks at an earlier time. The peak of the charge pulse, however, hardly shows any increase as the laser energy further increases and remains far below the space charge limit, which is about a factor of 5 larger than the maximum amplitude in the plot. Thus, it is the premature amplitude saturation, i.e., in comparison with the space charge limit, and the suppression of the later portion of the charge pulse that causes the observed charge limit (or charge saturation) behavior. Figure 4 shows a similar set of saturation plot and charge pulses measured at a different laser wavelength.

The suppression of the later portion of the charge pulses in the charge limit region suggests that as a large number of electrons are excited from the valence band into the conduction band under intense light illumination, the escape probability of the excited electrons is decreased. This points to an increase in the work function at the cathode's surface. A plausible scenario to cause a work function increase is the so called photovoltaic effect. As only a fraction of the electrons arriving at the surface successfully escape, there will be a large buildup of electrons at the surface under intense light illumination since the dissipation rate through recombination with holes is limited. The electrons discharge the surface and reduce the band bending in the surface region, thereby effectively raising the work function and causing the charge limit effect. Herrera and Spicer [5] have modeled the charge limit phenomenon based on the photovoltaic effect.

Figures 5 and 6 show the evolution of the charge saturation behavior as the QE of cathode 1 varies. Except for a reduced oversaturation effect in the charge limit region as the QE decays, the overall shape of the saturation curve remains primarily unchanged. In particular, it is noted that the laser pulse energy required to drive the cathode into charge limit remains about the same.

We now turn to the discussion on the results from cathode 2, whose doping concentration is a factor of 4 higher than that of cathode 1. Its QEs measured at 752 nm and 833 nm are comparable to those of cathode 1. Figure 7 shows a saturation plot along with charge pulses recorded at several laser pulse energies. In this case, there is no evidence of oversaturation in the charge limit region, which is in sharp contrast to the results of cathode 1. An examination of the charge pulses indicate that while indeed the charge pulse becomes narrower and peaks at an earlier time in the charge limit region, the later portion of the pulse is suppressed to a much smaller degree in comparison with the case of cathode 1. Apparently, this difference is related to the different doping concentrations in the two cathodes. A similar set of saturation plot and charge pulses measured at a different wavelength is shown in Figure 8, and the evolution of the saturation curve with varying QE is shown in Figures 9 and 10.

Accelerators often require closely spaced (in time) charge pulses for their high energy physics experiments. For example, the SLC/SLD requires two 2-nsec pulses separated by 60 nsec, while the conceptual Next Linear Collider require many more shorter and more closely spaced (about 1 nsec) pulses for every macropulse. It is therefore important to examine the interpulse effect from the standpoints of accelerator sources as well as fully understanding the charge limit phenomenon. Figure 11 shows two saturation plots of cathode 1 for pulse 2 with and without pulse 1 which is 56 nsec earlier [6]. The effect of pulse 1 on pulse 2 is rather significant considering the relatively long time separation. The effect is two-fold: a reduction in the photoemitted charge and an upperward shift of the laser energy for maximum charge in pulse 2. The upper panel of Figure 12 shows that the effect of pulse 1 on the amount of charge in pulse 2 monotonically decays with increasing time separation. The lower panel shows that the presence of pulse 1 mainly affects the amplitude of pulse 2 while leaving its pulse shape unchanged.

Figure 13 shows several sets of detailed interpulse effect data for cathode 1. Several conclusions may be drawn upon the data. (1) The harder the first pulse is pumped, the greater its effect on the second pulse. (2) The longer the wavelength (or the smaller the excitation photon energy) for pumping the second pulse, the greater the effect the first pulse has on the second one. (3) The time constant that characterizes the decay of the interpulse effect is on the order of 1 μsec, which is rather long. However, the interpulse effect for cathode 2 as shown in Figure 14 is strikingly different in that its decay time constant is orders of magnitude smaller than that of cathode 1. The interpulse effect is almost completely gone for time separations of >30 nsec. This contrasting behavior between the two cathodes, which differ only in doping concentrations, is correlated with their different intrapulse behaviors, i.e., the suppression of the later portion of the charge pulse (and also the degree of oversaturation) is much stronger for cathode 1 than for cathode 2. In the photovoltaic model, basically a single time constant that characterizes the dissipation rate of accumulated electrons at the surface can be used to describe both the interpulse and intrapulse effect. The strong dependence of the time constant on the doping concentration can be understood since the primary electron dissipation mechanism for our highly doped cathodes is holes tunneling to surface to recombine with the electrons [5]. This process is critically dependent on the width of the band bending region which is in turn controlled by the doping concentration. In fact, decay time constant as long as 25 sec has been reported for the surface photovoltaic effect in GaAs materials with a doping concentration of 1×10^{17} cm^{-3} or less [7].

Figure 15 shows that the charge limit for the 865 nm or 775 nm laser pulses is proportional to the QE measured at 752 nm or 833 nm. It is noted that, while the 865 nm charge limit line has a zero intercept with the ordinate, the 775 nm line does not. To aid theoretical understanding, it would be better to correlate the charge limit with the QE measured at the *same* wavelength, for QEs measured at different wavelengths do not exactly scale with one another as the cathode's

NEA condition deteriorates with time. Although Figure 16 shows that QEs measured at 752 nm and 833 nm scale reasonably well with each other, which imply that thermalized electrons contribute dominantly to the photoyield, care must be taken to generalize to any wavelength since the QE measured at very close to the bandgap threshold is more sensitive to changes in the surface NEA condition.

It is interesting to examine how the charge limit depends on the excitation wavelength. Figure 17 shows that the wavelength dependence of the charge limit is very weak for high QEs, and increases considerably as the QE deteriorates. It suggests that hot electrons (as opposed to thermalized electrons) become increasingly important in contributing to photoemission under the illumination of intense light as the surface work function rises.

Figure 18 shows that the logarithm of the QE depends linearly on the square root of the extraction electric field, which is consistent with the Schottky barrier lowering effect [8]. We may reasonably assume that the excited electrons that arrive at the cathode surface can be described by an effective temperature. Then, from the Schottky effect data the effective temperatures for the electrons excited with the 752 nm and 833 nm lasers may be easily determined to be 205 meV and 198 meV, respectively. The fact that the temperatures for the two cases are about the same implies that the photoexcited hot electrons are rapidly thermalized to the bottom of the conduction band and become hotter after traversing the band bending region to reach the surface. The slight wavelength dependence of the effective temperature may be attributed to incompletely thermalized electrons.

Finally, Figure 19 shows the charge limit as a function of the cathode bias. It is clear that the dependence is almost linear and, unlike in the case of QE, cannot be explained by the Schottky effect. Pulse shape measurements of the charge pulses indicate that the amplitude depends strongly on the cathode bias, which is responsible for the observed bias dependence of the charge limit. The fact that the charge limit does not simply depend on the cathode bias through QE, which is measured at low laser intensity, further illustrates the complicated nature of the charge limit.

In summary, we have studied the various aspects of the charge limit phenomenon. Charge limit is characterized by premature amplitude saturation, i.e., below the space charge limit, and suppressed emission in the later portion of the pulse. These two characteristics may be related and may simply be different manifestations of the same physics behind the charge limit phenomenon. The time constant for the charge limit effect to decay depends very sensitively on the doping concentration of a cathode. The strong dependence of the charge limit on the cathode bias points to the advantage of operating the electron source at the highest possible voltage if high intensity beams are desired.

* Work supported by DOE contract DE-AC03-76SF00515.

† Permanent address: Faculty of Science, Nagoya University, Nagoya 464-01, Japan.

REFERENCES:

1. D.C. Schultz, *et al.*, "Polarized source performance in 1992 for SLC-SLD", presented at the *10th Int. Sym. on H.E. Spin Physics,* Nagoya, Nov. 9-14, 1992.
2. J.E. Clendenin, *et al.,* "Performance of the SLC polarized electron source with high polarization", *Proceedings of the 1993 PAC Conference,* Washington, DC, May 17-20, 1993.
3. M. Woods, *et all.,* "Observation of a charge limit for semiconductor photocathodes", SLAC-PUB-5894, J. Appl. Phys., in press.

4. H. Tang, *et al.,* "Study of non-linear photoemission effects in III-V semiconductors", *Proceedings of the 1993 PAC Conference,* Washington, DC, May 17-20, 1993.
5. A. Herrera-Gomez and W.E. Spicer, "Physics of high intensity nanosecond electron sources", *Proc. SPIE's 1993 Int. Sym.,* San Diego, CA, July 11-16, 1993. SLAC-PUB-6307.
6. Due to certain instrumental problems, the charge in the second pulse is underestimated by about 5% in all of the double pulse measurements. Therefore, the actual charge in the second pulse should be scaled up by about 5%.
7. J. Qi, *et al.,* "Depletion-electric-field-induced changes in second-harmonic generation from GaAs", Phys. Rev. Lett. **71**, 633 (1993).
8. See, for example, S.M. Sze, *Physics of Semiconductor Devices,* p. 250-254, John Wiley & Sons, 1981.

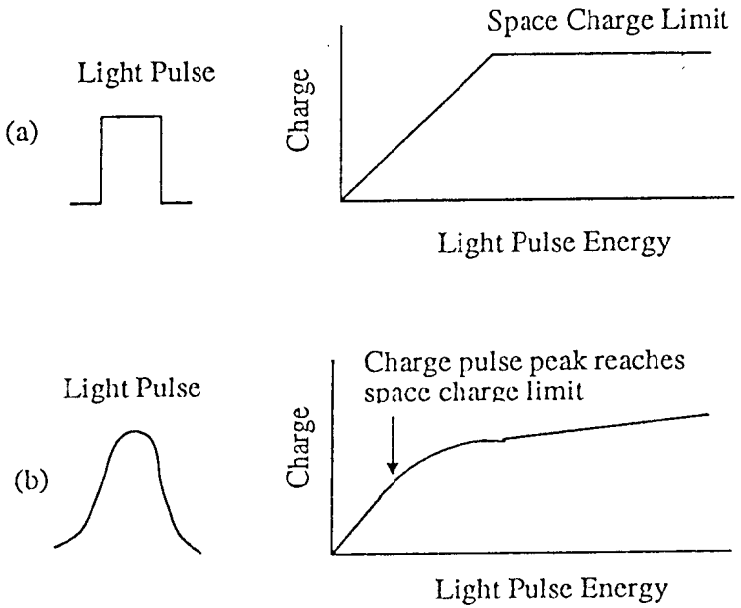

Fig. 1: Charge saturation behavior of an idealized linear-response photocathode illuminated with two types of light pulses.

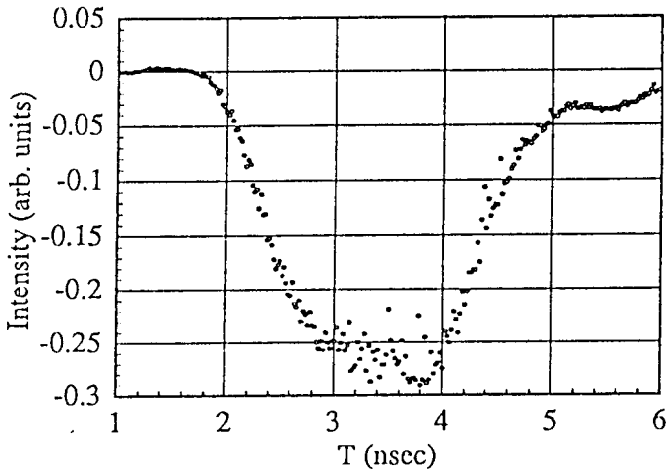

Fig. 2: Typical pulse shape of the 775 ns laser pulses used in the charge saturation studies.

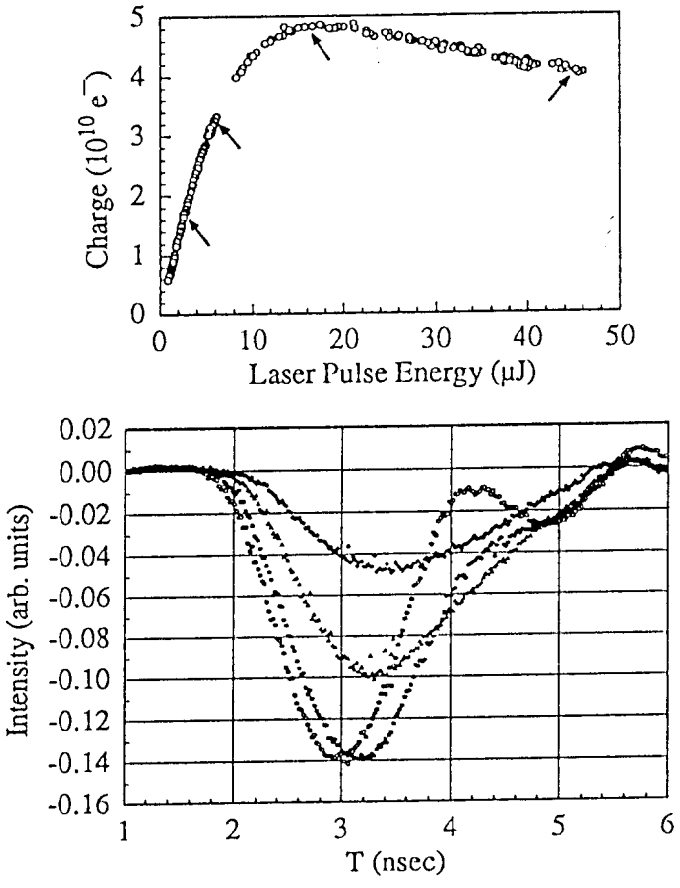

Fig. 3: Saturation plot and charge pulses for cathode 1 with 775 nm laser. The arrows indicate where the charge pulses are recorded. The QE at 833 nm is 0.38%.

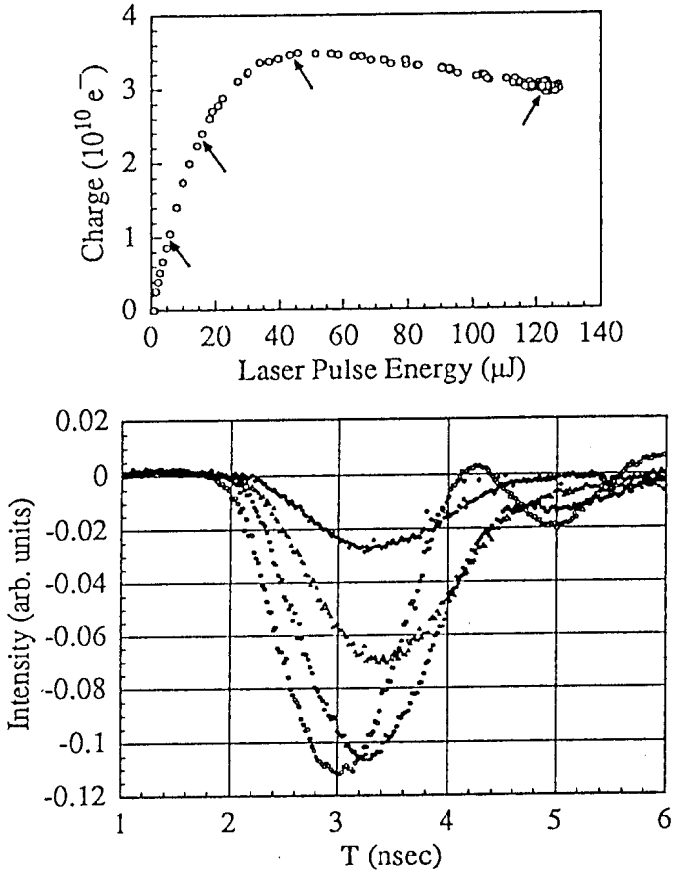

Fig. 4: Saturation plot and charge pulses dor cathode 1 with 865 nm laser. The arrows indicate where the charge pulses are recorded. The QE at 833 nm is 0.38%.

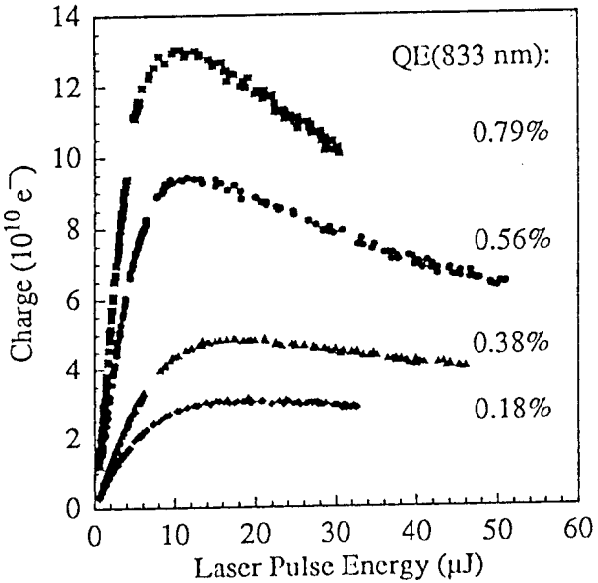

Fig. 5: Charge saturation data for cathode 1 with 775 nm laser pulses.

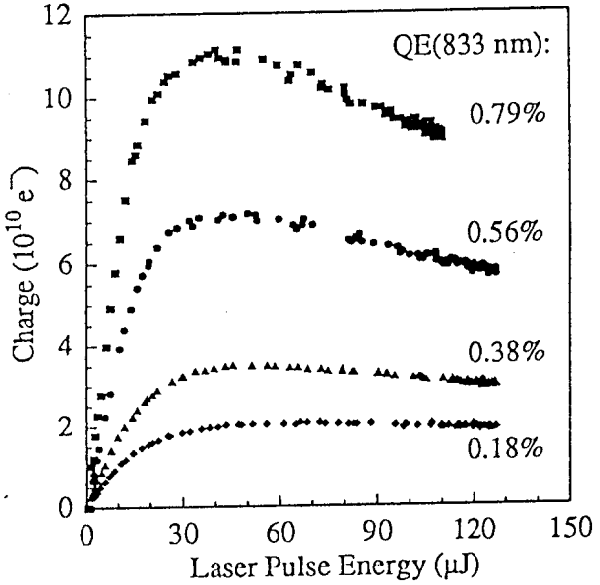

Fig. 6: Charge saturation data for cathode 1 excited with 865 nm laser pulses.

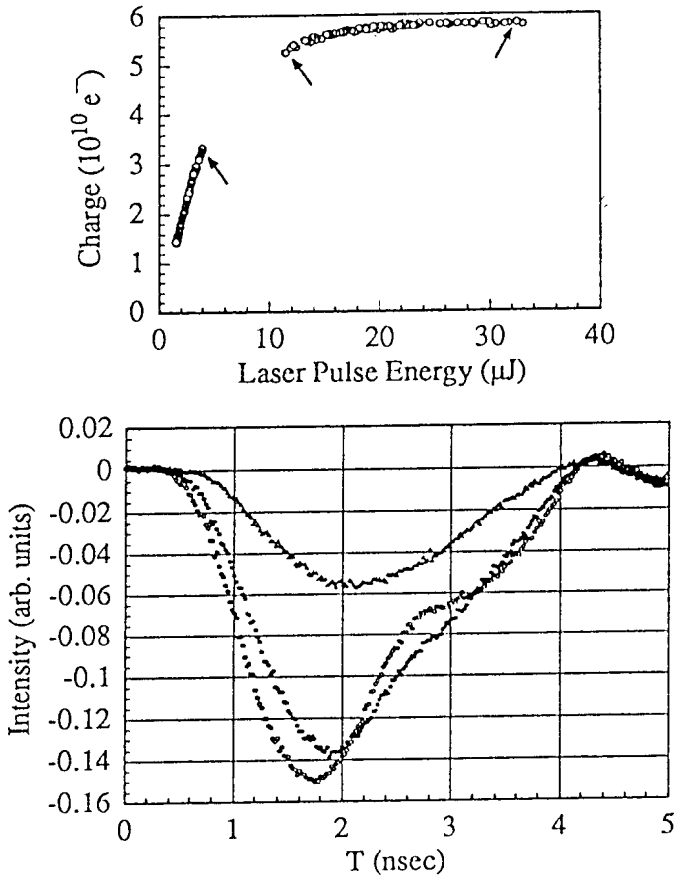

Fig. 7: Saturation plot and charge pulses for cathode 2 with 775 nm laser. The arrows indicate where the charge pulses are recorded. The QE at 833 nm is 0.24%.

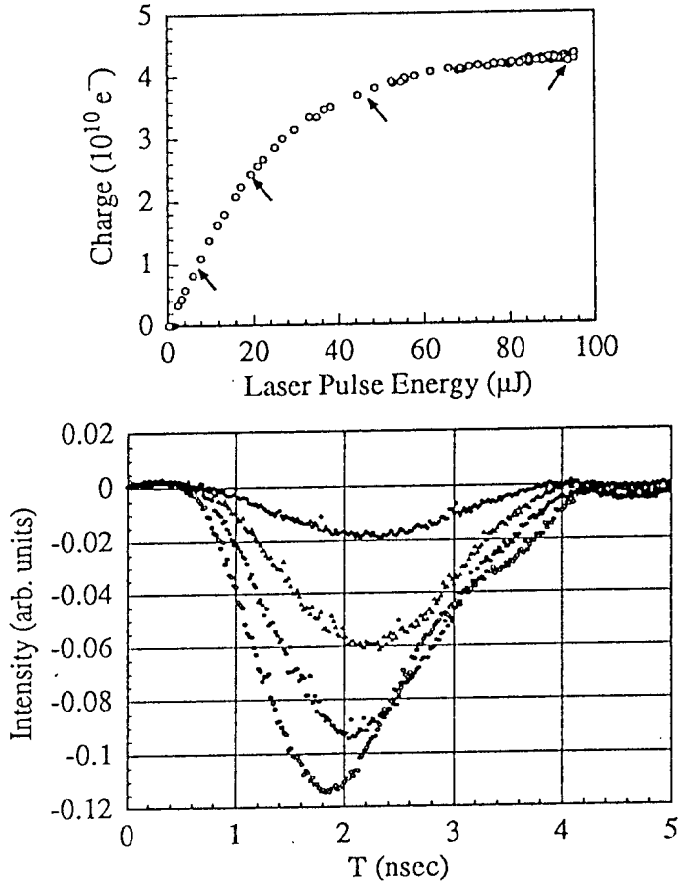

Fig. 8: Saturation plot and charge pulses for cathode 2 with 865 nm laser. The arrows indicate where the charge pulses are recorded. The QE at 833 nm is 0.24%.

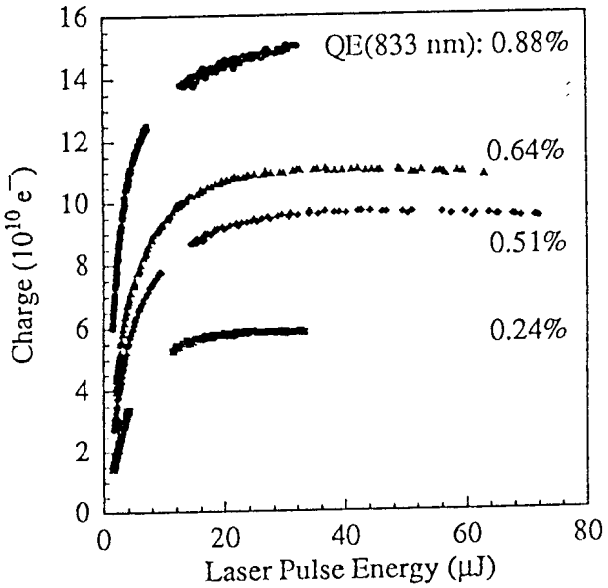

Fig. 9: Charge saturation data for cathode 2 excited with 775 nm laser pulses.

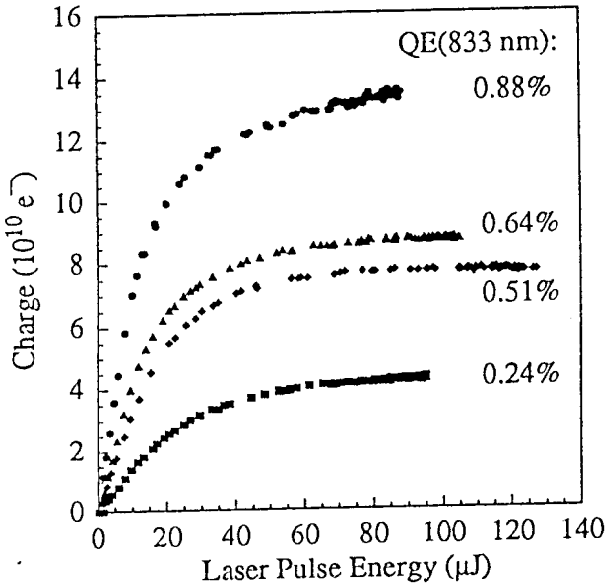

Fig. 10: Charge saturation data for cathode 2 excited with 865 nm laser pulses.

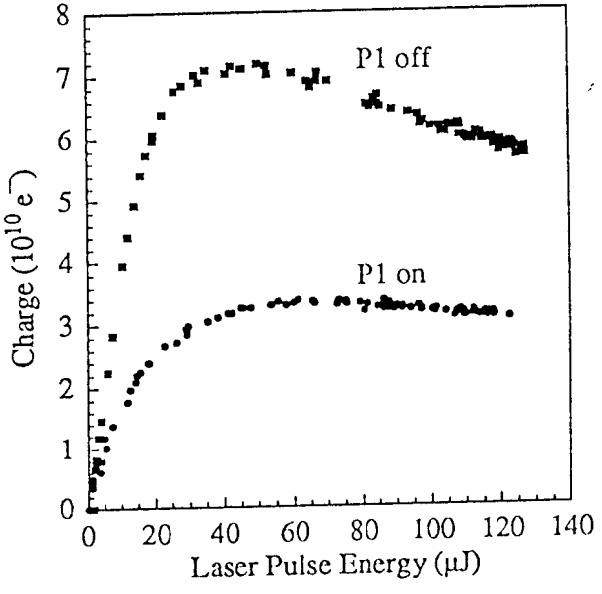

Fig. 11: Charge saturation data for the second pulse (P2) generated by 865 nm laser pulses with and without the first pulse (P1) generated 56 nsec earlier by 50 μJ 775 nm laser pulses for cathode 1.

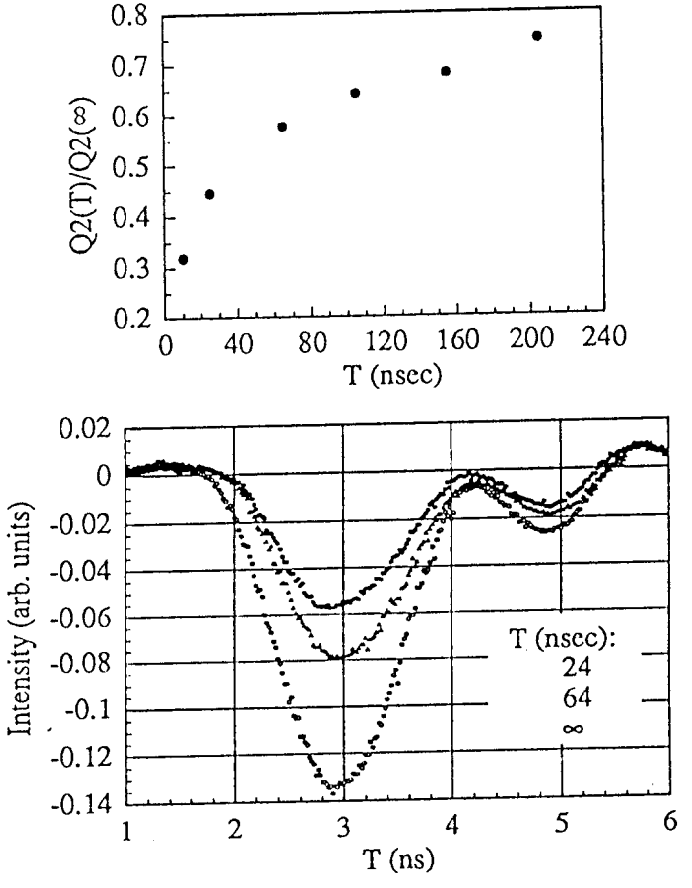

Fig. 12: Normalized charge in pulse 2 generated by 17 μJ 775 nm laser as a function of time delay from pulse 1 generated by 127 μJ 865 nm laser (upper panel) and charge pulses for pulse 2 (lower panel) for cathode 1. The QE at 833 nm is 0.34%.

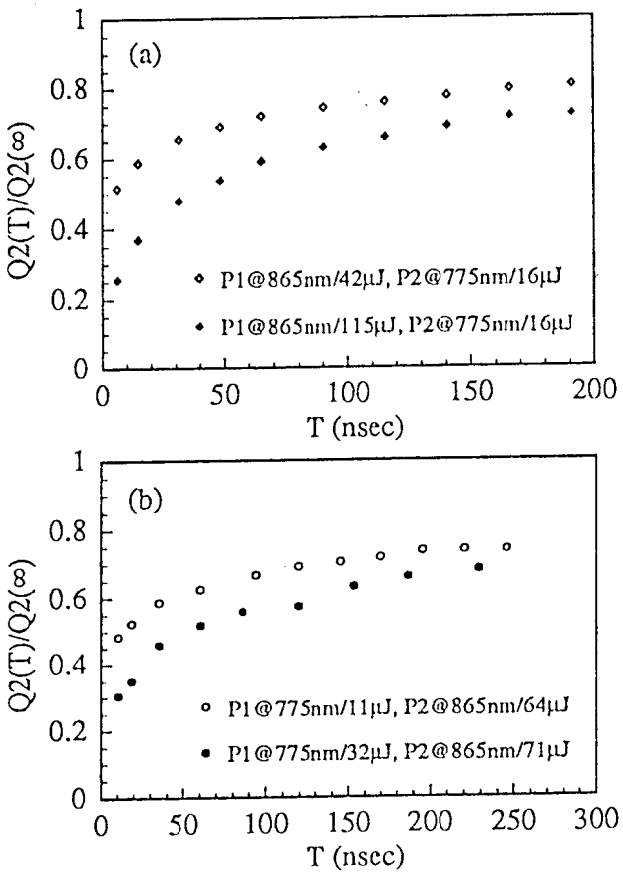

Fig. 13: Normalized charge in the second pulse (P2) as a function of time delay from the first pulse (P1) for cathode 1. The QE at 833 nm is 0.79% .

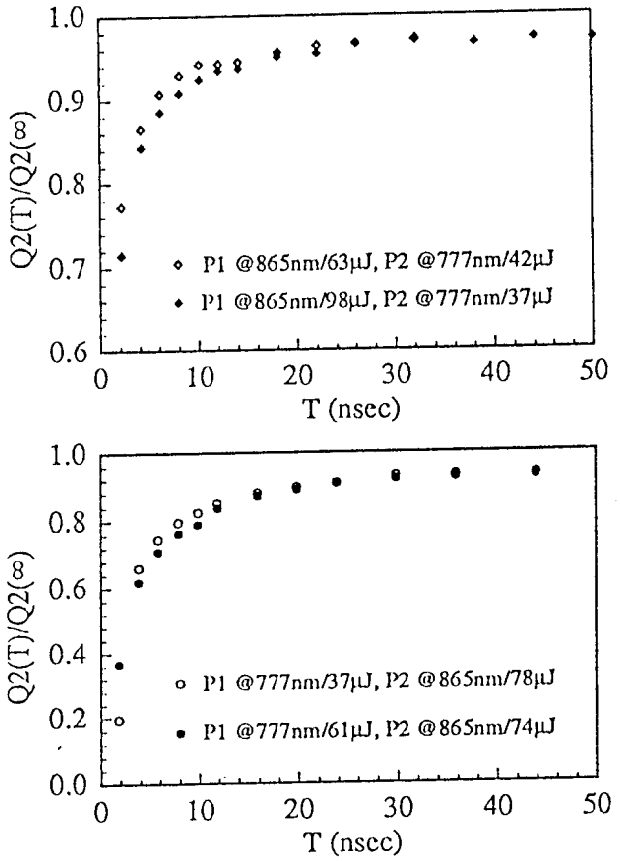

Figure 14: Normalized charge in the second pulse (P2) as a function of time delay from the first pulse (P1) for cathode 2. The QE at 833 nm is 0.34%.

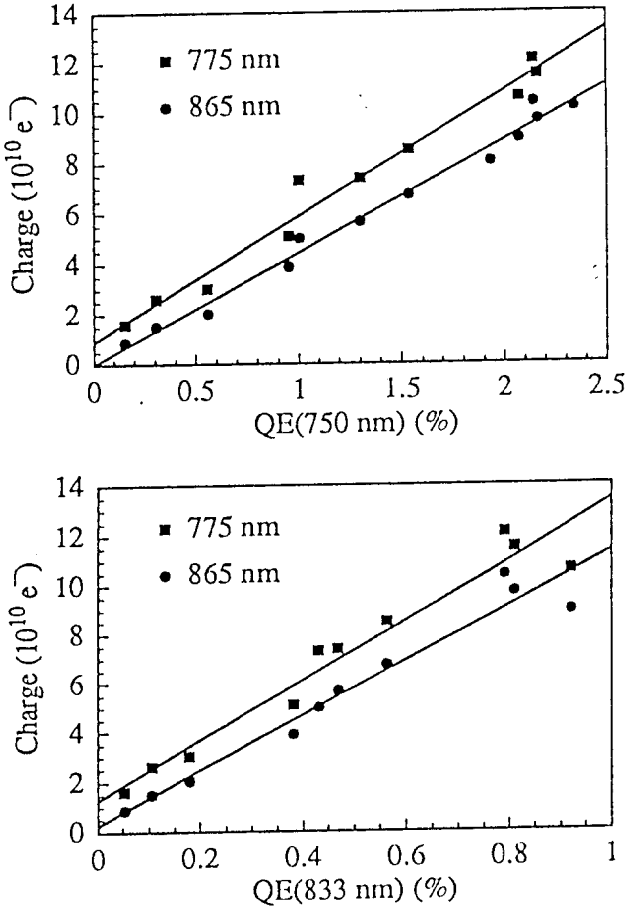

Fig. 15: Charge limit for 775 nm and 865 nm laser pulses as a function of QE. The lines are the best fit to the data.

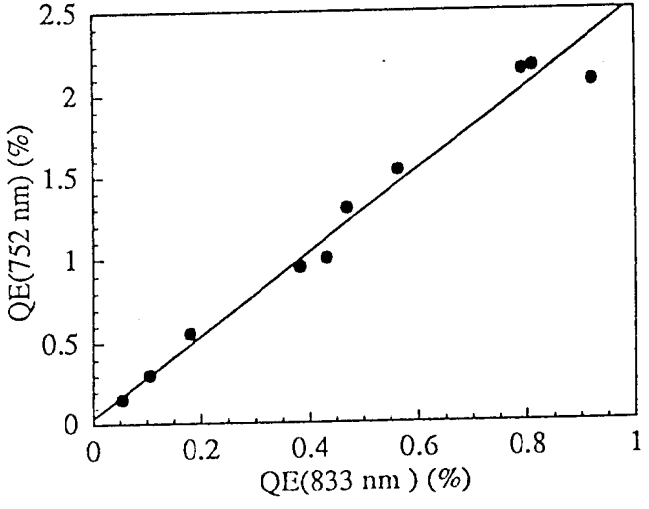

Fig. 16: QEs measured at 752 nm and 833 nm scale with each other reasonably well for cathode 1. The line is a best fit to the data.

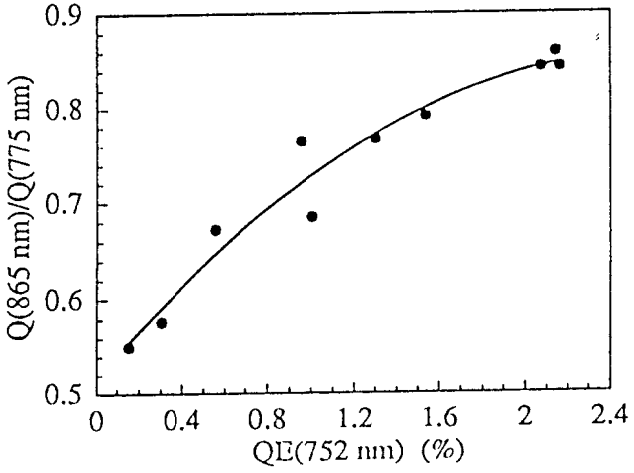

Fig. 17: Ratio of charge limits at 865 nm and 775 nm as a function of QE measured at 752 nm for cathode 1. The solid curve is a guide to the eye.

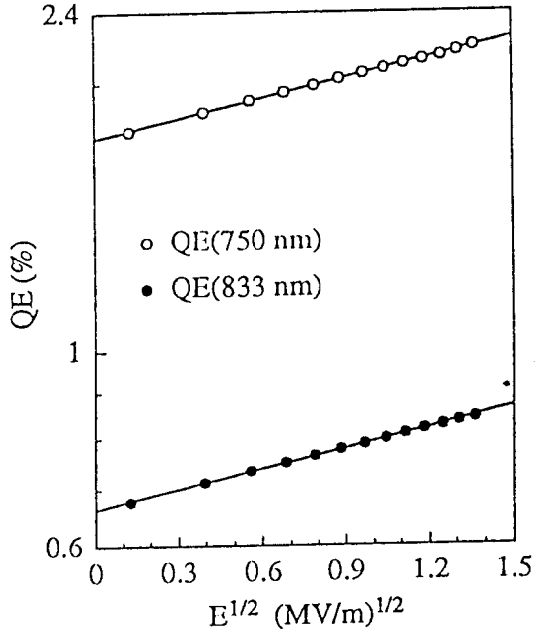

Fig. 18: QEs measured at 752 nm and 833 nm versus the square root of the extraction electric field for cathode 1. The lines are the best fit to the data.

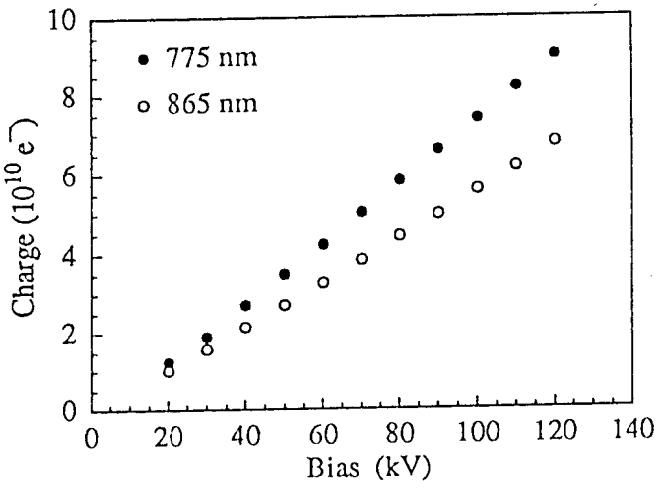

Fig. 19: Charge limit at two excitation wavelengths for cathode 2 as a function of cathode bias voltage.